Rhodobacter capsulatus Photoactive Yellow Protein: Genetic Context, Spectral and Kinetics Characterization, and Mutagenesis†

J. A. Kyndt,*,‡,§ J. K. Hurley,§ B. Devreese,‡ T. E. Meyer,§ M. A. Cusanovich,§ G. Tollin,§ and J. J. Van Beeumen‡

Laboratory of Protein Biochemistry and Protein Engineering, University of Gent, Ledeganckstraat 35, 9000 Gent, Belgium, and Department of Biochemistry and Molecular Biophysics, University of Arizona, Tucson, Arizona 85721

Received October 3, 2003; Revised Manuscript Received December 22, 2003

ABSTRACT: A gene for photoactive yellow protein (PYP) was previously cloned from *Rhodobacter capsulatus* (Rc), and we have now found it to be associated with genes for gas vesicle formation in the recently completed genome sequence. However, the PYP had not been characterized as a protein. We have now produced the recombinant RcPYP in *Escherichia coli* as a glutathione-S-transferase (GST) fusion protein, along with the biosynthetic enzymes, resulting in the formation of holo-RcPYP following cleavage of the GST tag. The absorption spectrum (with characteristic peaks at 435 and 375 nm) and the photocycle kinetics, initiated by a laser flash at 445 nm, are generally similar to those of *Rhodobacter sphaeroides* (RsPYP) but are significantly different from those of the prototypic PYP from *Halorhodospira halophila* (HhPYP), which has a single peak at 446 nm and has slower recovery. RcPYP also is photoactive when excited with near-ultraviolet laser light, but the end point is then above the preflash baseline. This suggests that some of the PYP chromophore is present in the cis-protonated conformation in the resting state. The excess 435 nm form in RcPYP, built up from repetitive 365 nm laser flashes, returns to the preflash baseline with an estimated half-life of 2 h, which is markedly slower than that for the same reaction in RsPYP. Met100 has been reported to facilitate cis−trans isomerization in HhPYP, yet both Rc and RsPYPs have Lys and Gly substitutions at positions 99 and 100 (using HhPYP numbering throughout) and have 100-fold faster recovery kinetics than does HhPYP. However, the G100M and K99Q mutations of RcPYP have virtually no effect on kinetics. Apparently, the RcPYP M100 is in a different conformation, as was recently found for the PYP domain of *Rhodocista centenaria* Ppr. The cumulative results show that the two *Rhodobacter* PYPs are clearly distinct from the other species of PYP that have been characterized. These properties also suggest a different functional role, that we postulate to be in regulation of gas vesicle genes, which are known to be light-regulated in other species.

Photoactive yellow protein (PYP) was originally isolated from *Halorhodospira halophila* (*1*, *2*). It is a small water-soluble cytoplasmic protein that is thought to be a blue-light photoreceptor in this organism. PYP has been reported in several other purple bacterial species, including *Rhodothallasium salexigens*, *Halochromatium salexigens*, *Rhodobacter sphaeroides*, *Rhodobacter capsulatus*, and *Rhodocista centenaria* (*3*−*6*). The *Rc. centenaria* PYP was found to be part of a larger polypeptide (Ppr) additionally containing phytochrome and histidine kinase domains. Gene deletion of *R. centenaria ppr* results in loss of light-induced regulation of a chalcone synthase homologue (*6*). We have also found that the genome sequence of *Thermochromatium tepidum* (Integrated Genomics) encodes a homologue of Ppr. However, the C-terminal domain comprises a presumed GGDEF/EAL type of diguanylate cyclase phosphodiesterase involved in the formation and/or hydrolysis of cyclic nucleotides (*7*).

Due to its structural and functional features, PYP is generally seen as the prototype for the PAS[1] domain family of signaling proteins, which has members in all kingdoms of life (*8*, *9*). The chromophore of PYP was shown to be a *p*-hydroxycinnamic acid thioester of cysteine 69 (*10*−*12*). The 1.4 Å crystal structure of HhPYP indicates that the chromophore is in the anionic trans conformation in the ground state of the protein (*13*). The photocycle is triggered by the absorption of blue light ($\lambda_{max} = 446$ nm) and initially results in a trans-to-cis isomerization, concomitant with the conversion of the ground-state P into I_0 (≤ 2 ps), and subsequently into $I_0^{\ddagger}$ (220 ps), both absorbing at 510 nm

† This work was supported by the Concerted Research Action, Grant 120C0198, of the "Bijzonder Onderzoeksfonds" of the University of Gent, and by the Fund of Scientific Research−Flanders, Project 3G042298, as well as by a grant from the National Institutes of Health, Grant GM 66146.

* Address correspondence to this author at Department of Biochemistry and Molecular Biophysics, University of Arizona, 1041 E. Lowell St., Tucson, AZ 85721. Tel.: (520) 621-5256. Fax: (520) 621-6603. E-mail: jkyndt@email.arizona.edu.

‡ University of Gent.

§ University of Arizona.

[1] Abbreviations: RcPYP*, recombinant *Rb. capsulatus* protein which has two extra residues at the N-terminus; PAS, acronym formed of the names of the first three proteins recognized as sharing this sensor motif (*p*eriodic clock protein of Drosophila, *a*ryl hydrocarbon receptor nuclear translocator of vertebrates, single-minded protein of Drosophila); GVP, gas vesicle protein; GST, glutathione-S-transferase; PCR, polymerase chain reaction; IPTG, isopropyl-β-D-thiogalactoside; ACN, acetonitrile; MES, 4-morpholine-ethanesulfonic acid; MOPS, 4-morpholine-propanesulfonic acid; Bicine, *N*,*N*-bis(2-hydroxyethyl)glycine; ORF, open-reading frame; WT, wild-type.

10.1021/bi035789f CCC: $27.50
Published on Web 01/30/2004

(*14*, *15*). $I_0^{\ddagger}$ converts to the red-shifted I_1 intermediate in about 3 ns (λ_{max} = 465 nm). In about 200 μs, the chromophore becomes protonated with loss of visible absorbance to form intermediate I_1', which rearranges in 3 ms (*9*) to I_2 (λ_{max} = 350 nm), a process accompanied by partial unfolding of the protein (*16*, *17*). The I_2 intermediate decays to the ground state with a lifetime of about 140 ms. In the convention we have adopted, I_2 is the final intermediate before recovery begins and is thought to be the signaling state.

A *pyp*-homologous gene from *Rhodobacter capsulatus* was cloned by Jiang and Bauer (*5*), and the genome sequence has now been nearly completed (*18*; www.Integratedgenomics.com), which allows determination of the genetic context of the PYP. Recently, we described the heterologous production of *Hr. halophila* PYP (HhPYP) in *Escherichia coli*, through coexpression of the biosynthetic genes from *Rb. capsulatus* (*19*). In the present study, we describe the use of the same biosynthetic system to heterologously produce *Rb. capsulatus* holo-PYP (RcPYP*). Initially, experiments failed to chemically reconstitute PYP following the procedure described by Imamoto et al. (*20*) and Genick et al. (*21*). After this problem was overcome by construction of a fusion protein, we purified holo-PYP and determined that the RcPYP* was, in some respects, quite different from HhPYP but has some of the spectroscopic and kinetic features of the *Rb. sphaeroides* PYP (RsPYP) (*4*, *22*). RsPYP differs from HhPYP in two very important respects: it displays a secondary peak at 360 nm that is both temperature and pH dependent, and the photobleached protein recovers 100-fold faster than HhPYP. This study was initiated to determine whether these characteristics are unique to RsPYP or define a distinct subgroup of the PYP family. The apparent discrepancy between rapid kinetics of recovery of the RsPYP and the amino acid sequence, which suggests that it and the RcPYP should be slower than HhPYP, was addressed by site-directed mutagenesis of the RcPYP.

MATERIALS AND METHODS

Plasmid Construction. All molecular cloning experiments were performed according to Sambrook et al. (*23*). The *pyp* gene from *Rb. capsulatus* (DSMZ 1710, type strain) was cloned into the pGEX-4T-2 vector (Amersham Biosciences, Uppsala, Sweden) as a downstream fusion with the gene for glutathione-S-transferase (GST), since expression of the *pyp* gene alone led to insoluble protein. The following primers were used for PCR amplification of the *pyp* fragment: BamHIPYP (CGGGATCCATGGAAATCATTCCGTTCGG) and PYPNotI (GGAAAAAAGCGGCCGCT CAGGCCCGCTTCAGGAAG). *Bam*HI and *Not*I restriction sites (underlined) were introduced into the *pyp* gene, allowing us to clone it in frame with the *gst* sequence of the pGEX-4T-2 vector. This resulted in the pGEX-4T(pyp) construct, which has a ColE1 origin of replication and a carbenicillin resistance-encoding gene. The *gst* and *pyp* are separated by a 24-bp region that encodes a thrombin recognition site (SDLVPRGS, where cleavage is between Arg and Gly). The RcPYP is one residue shorter than HhPYP and the recombinant protein is two residues longer than wild-type (including the initiator Met), which we will designate RcPYP*. To avoid confusion, we will also use the HhPYP numbering throughout.

Mutagenesis Experiments. The Quick Change PCR mutagenesis kit (Strategene) was used to create the K99Q and G100M mutants. The pGEX-4T(pyp) construct served as template, in a PCR reaction with the following primers: for PYPG100M, TCAATTACAAGATGGCCGAAGTGG (and complement as reverse primer), and for PYPK99Q, CAATTACCAGGGCGCC (and complement as reverse primer). The mutated bases are underlined. The reaction was performed following the instructions of the manufacturer, but additional elongation times (up to 6 min/kb for 20 cycles) had to be applied to achieve enough product. The mutated genes were expressed and the resulting proteins purified in a manner analogous to that described below for the wild-type. Mutagenesis was confirmed by DNA sequencing of the genes and molecular mass analysis of the purified proteins.

Protein Expression and Purification. Escherichia coli BL21(DE3) Star was transformed with both pGEX-4T-2(pyp) and pACYC(talpcl) by the use of electroporation. The latter plasmid, containing the genes for the biosynthetic enzymes, was described earlier (*19*). One-liter cultures of co-transformants were grown at 28 °C on carbenicillin (Cb, 100 μg/mL) and chloramphenicol (Cm, 25 μg/mL) as antibiotics. When the cells reached an OD_{600} of approximately 0.7, they were induced with IPTG to a final concentration of 0.5 mM. After 16 h of induction, the cells were pelleted by centrifugation. Pellets were resuspended in 10 mL of Tris-HCl buffer (20 mM, pH 9.0) and fractionated by two freeze−thaw steps, followed by sonication. After centrifugation, the supernatants were dialyzed and loaded onto a 10 mL Q-Sepharose fast-flow column (Amersham Biosciences). Elution was performed using Tris-HCl buffer (50mM, pH 9.0) with increasing NaCl (with steps of 50 mM, 100 mM, 250 mM, 350 mM, 500 mM, and 1 M). The GST-PYP eluted mainly with 250 mM NaCl. After concentration of the yellow-colored fractions on Ultrafree-15 centrifugal filters (Millipore, Bedford, MA), the sample was applied to a Superdex 75 size exclusion column (Hiload 16/60, Amersham Biosciences), which was connected to an ÄKTA explorer HPLC system (Amersham Biosciences). The running buffer consisted of 100 mM Tris-HCl, pH 9.0, supplemented with 100 mM NaCl. After this step, the yellow samples were concentrated on Ultrafree-15 centrifugal filters. The GST-PYP fusion protein was digested with thrombin (Sigma-Aldrich, St. Louis, MO) for about 16 h at 15 °C in Tris-HCl buffer, pH 8.5, and 50 mM NaCl. Using these conditions, approximately 5 μg of protein was cleaved with 1 unit of thrombin. Samples of the cleavage reaction were taken at several time intervals and analyzed on SDS−PAGE to ensure that the reaction had gone to completion. Subsequently, the size exclusion step was repeated as described above to separate PYP from GST. At this point the PYP had a purity above 95%, based on Coomassie brilliant blue stained gels, with a yield of 1 mg of holo-PYP per liter of culture. The filter-sterilized protein was indefinitely stable at 4 °C.

Mass Spectrometry. Molecular mass analysis was performed on a Q-TOF mass spectrometer (Micromass, Manchester, UK) equipped with a nano-electrospray source. Approximately 5−10 pmol of protein was dissolved in 5 μL of 50% ACN/0.1% HCOOH and loaded into a nanospray capillary. RcPYP contains two cysteine residues, either of which might

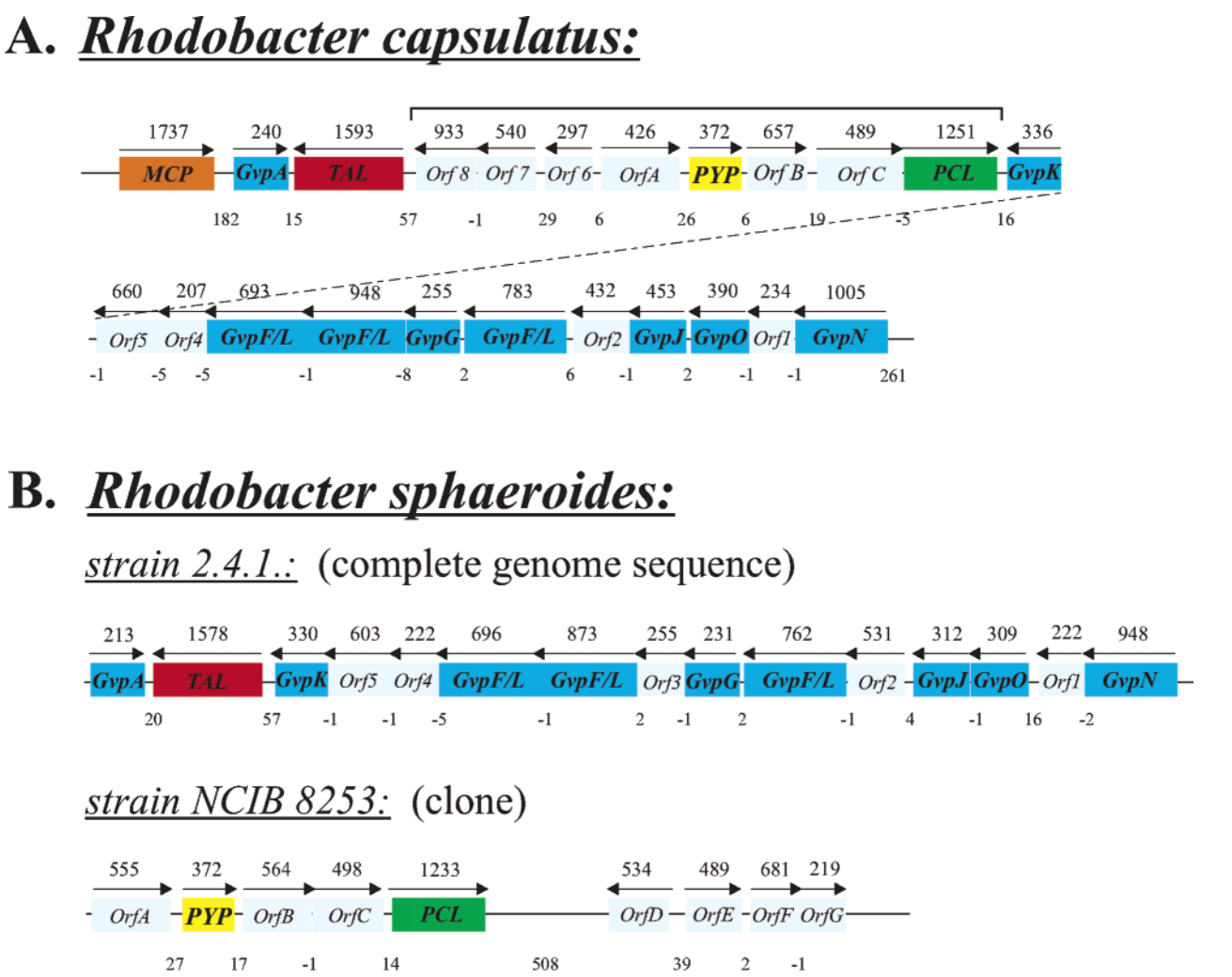

FIGURE 1: Genomic organization around the *pyp* gene in *Rb. capsulatus* (A; 15,5 kbp fragment). The orientation of each gene is indicated by arrows, and the gene size (bp) is indicated on top and the intergenic region (bp) below the gene. Genes that show homology to *gvp* genes are marked in blue. In the *Rb. sphaeroides* genome (B), the *gvp* genes show the same distribution, but the PYP and pCL-containing region between TAL and *gvpK* (marked with a black line above the sequence) is lacking. The *Rb. sphaeroides pyp* and surrounding genes, reported from strain NCIB 8253 (*4*), are also presented.

bind chromophore. To identify the chromophore-binding residue, the holo-PYP was digested with trypsin in 50 mM NH_4HCO_3 for 4 h. The ratio of trypsin to holo-PYP was 1:40 (w/w). The peptide mixture was directly submitted to nano-electrospray without prior purification. Peptides were fragmented with collision- induced dissociation using argon as the collision gas.

UV/Vis Spectroscopy. Absorption spectra were obtained by using a UVIKON spectrophotometer (Kontron, Herts, UK). Samples were measured in Tris buffer at varying concentrations and pH, or in universal buffer (20 mM MES/MOPS/Bicine), according to the preceding purification step.

Time-Resolved Spectroscopy. The laser flash photolysis apparatus and data analysis protocol were as described previously (*2*, *24*).

RESULTS

Rb. capsulatus pyp and Its Genomic Organization. The organization of *pyp* and its two biosynthetic genes in the *Rb. capsulatus* genome is shown in Figure 1. The two biosynthetic genes, *tal* and *pcl*, are in close proximity to the *pyp* gene. Furthermore, these three genes are flanked by those for gas vesicle formation. Gas vesicles are flotation devices that bring cells to the surface of the water, where light and oxygen are abundant. Gas vesicles are known to be induced at low light intensities and repressed at high intensities in some species. Because PYP is a light sensor, it is plausible that it could be involved in regulation of the gas vesicles. Homologues to all of the *gvp* genes minimally required for the formation of gas vesicles in halobacteria (*25*) are present, although a *gvpC* homologue, which is involved in providing strength and shape to the gas vesicles, has not been found. The genes appear to be organized in at least four different transcriptional units. *Pyp*, *pcl*, and three other genes are oriented in one direction, whereas *tal* and three other ORFs are oriented in the opposite direction upstream of PYP. *GvpN* through *gvpK*, including 10 other genes, are all oriented in the same direction, but downstream of and opposite to *pyp*. *GvpA*, which encodes the main structural unit of the gas vesicle, is immediately downstream of *tal* in the opposite orientation.

Although we found no *pyp* homologue in the complete *Rb. sphaeroides* genome sequence (Joint Genome Institute, strain ATH 2.4.1), the gas vesicle genes seem to be present in the same orientation as in *Rb. capsulatus*, and one of the biosynthetic enzymes of PYP (*tal*) is clustered with them

(Figure 1). The RsPYP was cloned from strain NCIB 8253 (4). It is likely that the absence of *pyp* in *Rb. sphaeroides* strain 2.4.1 is due to deletion through many years of nonselective cultivation in the laboratory.

Heterologous Production of holo-PYP.* After amplification of the *pyp*-homologous ORF from *Rb. capsulatus* (strain DSMZ 1710), the DNA fragment was sequenced and found to be the same as that available on the Internet (www.Integratedgenomics.com). An alignment of the RcPYP translated sequence with the previously characterized PYP's can be found in the work of Jiang et al. (*6*). There is 38% identity between the RcPYP and those from the halophilic species, *Hr. halophila*, *Rt. salexigens*, and *Hc. salexigens*, but the largest identity was found with the PYP sequence from *Rb. sphaeroides* (76%).

The *Rb. capsulatus pyp* gene was cloned into the high-copy pGEX-4T-2 expression vector. The resulting pGEX-4T(pyp) allows tightly inducible expression of the apo-PYP gene with *gst* fused to the 5′ end. The reason for using this fusion construct was to improve the solubility of the produced PYP and to facilitate reconstitution with chromophore. Expressing the *Rb. capsulatus pyp* without the fused *gst* (using pET11a and pET15b vectors) resulted in the production of 90−95% of the apo-PYP as insoluble protein. The fusion with GST improved the solubility of the apo-PYP up to an estimated 60% of the total (data not shown).

The cloned genes encoding the two biosynthetic enzymes of PYP were described earlier (*19*). The pACYC(talpcl) plasmid was cotransformed with pGEX-4T(pyp) into *E. coli* BL21(DE3) Star. After induction of cotransformants containing all three genes, the holo-PYP* was purified from *E. coli*. The yield of GST-RcPYP after the first anion-exchange step on a Q-Sepharose FF column was significantly lower than the yield reported for the HhPYP when the heterologous production system was used. This appears to be a consequence of instability of RcPYP during purification.

After purification by size exclusion, the protein was cleaved with thrombin to remove the GST-tag. After overnight digestion, all of the GST-PYP was cleaved into GST and PYP*. There was no change in the absorption spectrum of the PYP* after removal of the GST, except at 280 nm where GST absorbs. This indicates that the effect of the GST tag on the PYP* conformation is negligible. To separate the PYP* from GST after cleavage, a second size exclusion step was performed. At that point purity was greater than 95%. However, when the protein was frozen at −20 °C and thawed, about half of the purified RcPYP did not redissolve, which reflects its instability.

Mass Spectrometry. To ascertain that the GST-PYP had a single *p*-hydroxycinnamic acid chromophore covalently bound to the protein as opposed to binding at both cysteines (C69 and C118), we analyzed the partially purified protein by mass spectrometry. In the first step of purification, the protein mass was measured in its denatured state by use of an electrospray Q-TOF mass spectrometer. The observed mass was 40 390 Da, which is 147 Da larger than the theoretically calculated mass of the GST-apo-PYP, but identical to GST-holo-PYP, consistent with a single chromophore covalently bound to the polypeptide. There was no evidence of any protein lacking the chromophore, or any doubly reconstituted species, nor is it likely that these species would have been separated at such an early stage of purification. The fact that no apo-PYP could be detected at this point is different from what was found for the HhPYP (*19*), where an apo-PYP fraction was removed only after additional purification.

Since the RcPYP sequence contains Cys residues at positions 69 and 118 (in contrast to HhPYP, which has only C69), we investigated to which of these residues the *p*-hydroxycinnamic acid is attached. This was done by digesting the protein with trypsin and analyzing the resulting peptides by MS/MS. The extra 147 Da was associated with the peptide that contains the C69 residue. This experiment clearly showed that all of the chromophore was attached to C69 and not to the cysteine residue at position 118.

Mass analysis of the thrombin-cleaved PYP* showed that the protein contains an extra GlySer dipeptide, as was expected considering that the thrombin cleavage site was not engineered precisely at the N-terminus of PYP. N-terminal sequencing of the first six residues (GSMEII...) also confirmed the presence of these additional two residues. Neither mass spectrometry nor N-terminal sequencing showed any evidence for different N-termini that might have resulted from incorrect cleavage by thrombin.

Spectral Characterization. The absorption spectrum of purified RcPYP* is shown in Figure 2. Besides the absorbance peak at 435 nm, which is similar to the 446 nm peak for Hh and RsPYPs, there is a relatively large absorbance with an estimated maximum at 375 nm. This spectrum was unaffected by overnight incubation in the dark or by exposure to room light. At first sight, the absorption spectrum resembles that of the Y42F mutant of HhPYP (*26*−*28*). In this mutant, a 391 nm spectral shoulder on the 458 nm maximum, due to a second, less stable chromophore conformation in the ground state, was found to be pH- and temperature-dependent and strongly affected by chaotropes and kosmotropes (*27*). The 375 nm peak of RcPYP* is relatively larger than the 360 nm peak of RsPYP (under the same conditions of pH and temperature). This may account in part for the shift of the characteristic 446 nm peak of Hh and RsPYP to 435 nm in RcPYP*. The 375 to 435 nm ratio of RcPYP* is 1.04 in Tris-HCl (pH 8.0) at room temperature.

It had previously been shown that the 446 nm peak of RsPYP increases in magnitude with increasing temperature while the 360 nm peak decreases (*4*). The same was found to be true for RcPYP* in the 5−30 °C range, as can be seen in Figure 2A. At 5 °C, the 375 nm peak is relatively larger, while above 20 °C, the 435 nm peak is increased above the 375 nm maximum. This temperature effect, with an isosbestic point at 415 nm, was found to be reversible at least up to 25 °C but, at temperatures above 30 °C, a slight, irreversible denaturation of the protein occurs which further increases with temperature. Such a thermal effect was not observed for HhPYP, whose 446 nm absorption peak was not significantly changed by temperature up to about 80 °C (*29*, *30*).

It was reported that the RsPYP spectrum is dependent on pH (*4*). The pH effect was fit with two p*K*'s, at 6.5 ($n = 1$) and 3.8 ($n = 2$). The 446 nm form is favored at pH values above 6.5, and the 360 nm form is favored at pH values between 6.5 and 3.8, below which the protein is converted to a 345 nm form, corresponding to the absorbance of denatured protein. When a similar experiment is performed with RcPYP*, the protein begins to precipitate irreversibly

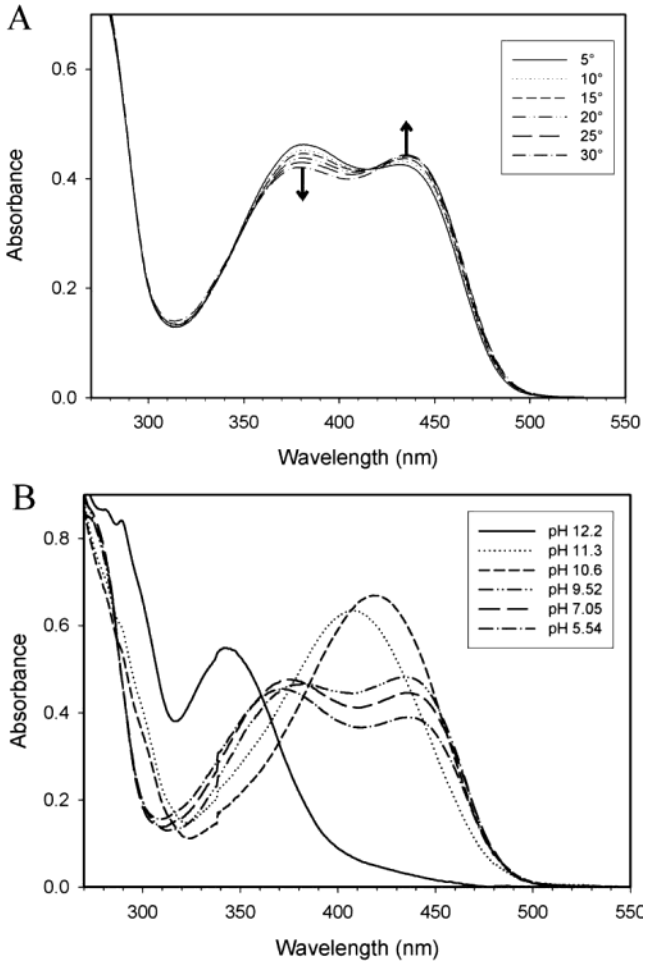

FIGURE 2: (A) Temperature dependence of the absorption spectrum of RcPYP*. While the temperature is increased from 5 to 30 °C, the magnitude of the 375 nm peak decreases and that of the 435 nm peak increases. At higher temperature, irreversible protein denaturation becomes significant and interferes with the experiment. The thermal experiment was performed in universal buffer (20 mM MES/20 mM MOPS/20 mM Bicine) at pH 9.0. The relatively large absorption at 260 nm is due to the buffer (the ratio of 280 to 435 nm absorbance of pure protein is actually 1). (B) pH dependence of the absorption spectrum of RcPYP*. Increasing the pH from 5.5 to 10.6 leads to an increase of the 435 nm absorption. It can also be seen that, above pH 10, both the 435 and the 375 nm forms are replaced by a single form with an absorption maximum at 420 nm at pH 10.6, and at 410 nm at pH 11.3. At pH 12 the maximum shifts toward 345 nm, which corresponds to the fully denatured form. All measurements were performed in universal buffer.

below pH 5.5. However, above pH 5.5, a similar increase of the 435 nm form could be observed (Figure 2B). Upon further increasing the pH to 10.6, only a single absorption peak is visible with RcPYP*, which absorbs at 420 nm. This peak gradually shifts to shorter wavelengths with increasing pH, which is indicative of denaturation and base-catalyzed hydrolysis of chromophore. Above pH 11.0, the protein begins to precipitate, while the wavelength maximum reaches a value of 345 nm, and practically no 435 or 420 nm absorption is left. From these experiments and those with RsPYP, it appears that, at both low pH (below pH 4) and high pH (above pH 10.5), a new species with a single characteristic absorption at 345 nm can be formed with the *Rhodobacter* PYPs. These forms most likely correspond to protonated and/or free hydrolyzed chromophore. However, the pH 10.6, 420 nm form is like the alkaline spectral forms of HhPYP, as described by Meyer et al. (*28*), which were ascribed to the ionization of E46.

The effect of chaotropes and kosmotropes on the spectrum of HhPYP mutant Y42F was reported by Brudler and coworkers (*27*). The 458 nm peak was shown to be favored in the presence of kosmotropes such as ammonium sulfate, but the 391 nm form was favored in the presence of chaotropes such as ammonium chloride. At high concentrations of chaotrope, the 391 nm form was converted to a 350 nm species. To investigate whether the 375 nm peak of RcPYP* behaves in a similar way, we studied the changes in its absorption spectrum in the presence of the same ammonium salts. Figure 3A shows the effect of the chaotrope NH_4Cl, in which the 435 nm form dramatically diminishes without changing its wavelength maximum, as shown in Figure 3B, while the 375 nm form is favored and gradually shifts its maximum toward 350 nm, as shown in Figure 3C. At a concentration of 4 M NH_4Cl, some of the protein was lost due to precipitation. The effect of the kosmotrope, ammonium sulfate, which is known to make proteins more compact by salting out hydrophobic residues, is given in Figure 4. Although precipitation of the protein above 1.0 M $(NH_4)_2SO_4$ interferes with the measurement, it can clearly be seen that there is a relative increase in the absorption of the 435 nm form.

Photocycle Kinetics. To investigate the kinetics of the photocycle and the nature of the 375 nm absorption peak, we performed microsecond laser flash photolysis experiments with RcPYP*. In HhPYP, there is a biphasic bleach of absorbance at 446 nm, followed by recovery. In RcPYP*, a similar kinetic pattern was observed, although both the second bleach phase and the recovery kinetics at 435 nm are faster than in HhPYP (*2*, *21*) by factors of 10 and 100, respectively, as shown in Figure 5. The fastest phase of bleach is beyond the time resolution of the instrumentation we used and was not measured. An analogous result was seen with the RsPYP, where bleach and recovery are faster than in HhPYP (*4*). Table 1 gives the bleach (corresponding to $I_1 \rightarrow I_2$) and recovery ($I_2 \rightarrow P$) kinetics with several excitation and detection wavelengths. We also examined the time-resolved difference spectra (in the 390−550 nm region). The first excitation wavelength we tested was 445 nm. The amplitude for the faster formation of I_1 (complete in <20 μs) and slower (200 μs) bleach to form I_2 was plotted as shown in Figure 6. Concomitant with the expected bleach of the 435 nm form, there appears to be minor bleaching of a component in the 390−410 nm region, which can be seen as a shoulder on the 435 nm bleach. This may correspond to bleaching of a component in the 375 nm band. This shoulder was not observed in the RsPYP difference spectrum (*4*), but that may be due to the smaller contribution of the intermediate spectral form to the ground-state spectrum and to its wavelength maximum at 360 nm, which is similar to that of bleached protein.

The pH dependence of the RcPYP* recovery reaction is shown in Figure 7. Only small changes in the rate of recovery could be detected between pH 5.6 and 9.4. This is similar to but less pronounced than the case for HhPYP, where there was also a bell-shaped pH dependence (*21*), but with markedly different amplitudes (700−890 s^{-1} for RcPYP* and 0−6.3 s^{-1} for HhPYP). The pH dependence for RsPYP was not reported. The pK_a values calculated for RcPYP* (pK_1

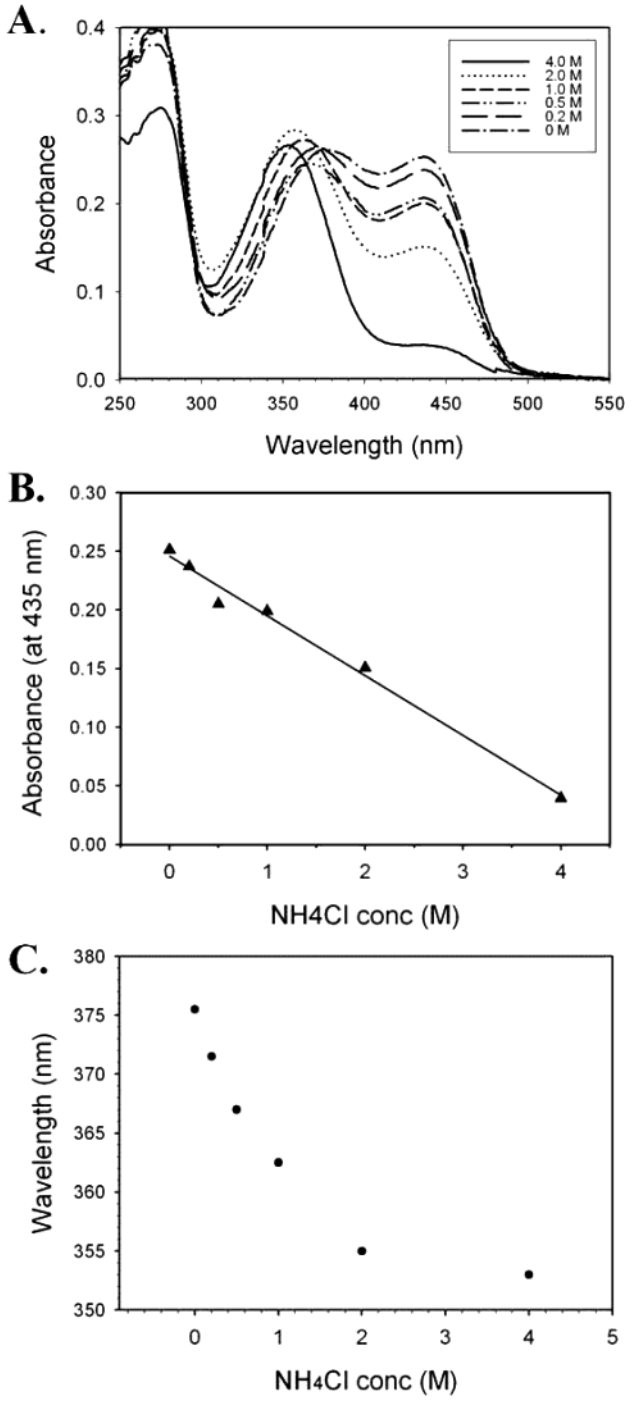

FIGURE 3: (A) Effect of increasing concentration of the chaotrope NH_4Cl on the absorption spectrum of RcPYP* in Tris-HCl (50 mM, pH 8.0) at 20 °C. (B) The 435 nm maximum as a function of NH_4Cl concentration. (C) The continuous change in absorption maximum of 375 nm to 350 nm as a function of NH_4Cl concentration.

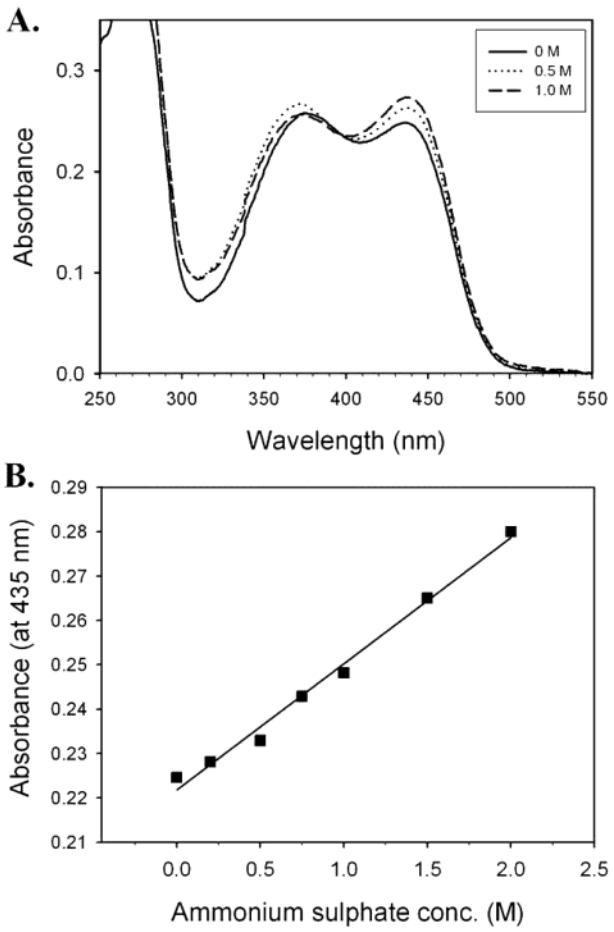

FIGURE 4: (A) Effect of increasing the concentration of the kosmotrope $(NH_4)_2SO_4$ on the absorption spectrum of RcPYP* in Tris-HCl (50 mM, pH8.0) at 20 °C. (B) The 435 nm absorbance as a function of the salt concentration.

$= 6.7$ and $pK_2 = 9.6$) are comparable to the values for HhPYP ($pK_1 = 6.4$ and $pK_2 = 9.4$), which suggests that the same groups are responsible for the pH dependence of the recovery reaction. These were reported to be due to the E46 carboxyl and the chromophore hydroxyl in the photobleached protein (*28*). The highest value of the recovery rate for the RcPYP* was at pH 8.1 ($k = 890 \pm 30$ s^{-1}), similar to the optimum of pH 8 for HhPYP. As stated above, the protein tends to precipitate below pH 5.5 and to be converted to another spectral form above pH 9.5, which precludes measurements outside that range.

To determine whether the 375 nm absorbance peak of RcPYP* is also photoactive, we excited the protein with 386 nm light, which is between the two maxima at 375 and 435 nm and which should excite both bands. The rates of recovery at 435 nm are in the same range as with 445 nm excitation, where only the 435 nm peak should be active (see Figure 8A and Table 1). This indicates either that only the 435 nm band is bleached and subsequently recovers or that the kinetics are essentially the same for the two species. However, the recovery of 435 nm absorbance returns to a new baseline, which is significantly higher than the preflash baseline. The ratio of "recovery above baseline" to bleach is 0.24. A difference spectrum with time points taken around 9 ms after the bleach also shows that there is formation of the 435 nm form at the expense of the 375 nm form (data not shown).

In the experiments of Figure 8A, where we used light excitation at 386 nm, there was still bleaching at 435 nm which, as stated above, may have been due to spectral overlap. To minimize the effect of the spectral overlap, we used a different laser dye to excite the sample at 365 nm. The rate constants at 435 and 375 nm for 365 nm excitation are given in Table 1, while the recovery kinetics at both wavelengths are shown in Figure 8B and C. The rate of recovery at 375 nm is higher (approximately 1100 s^{-1}) than what we had seen at 435 nm (approximately 600 s^{-1}). This might indicate that RcPYP* is able to perform two photo-

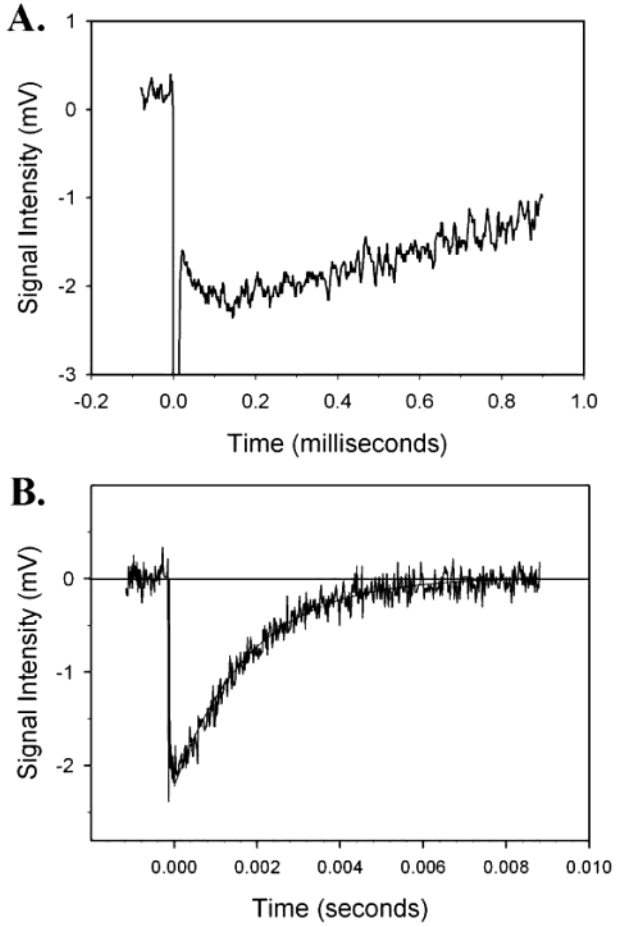

FIGURE 5: (A) Bleach and (B) recovery of RcPYP* measured at 435 nm, after excitation with 445 nm laser light (at time 0). The prominent negative spike in panel A is a laser artifact. The sample contained RcPYP* with an absorption at 435 nm of 0.2. Measurements were performed at pH 8.0 in universal buffer. Kinetic values derived from these plots are given in Table 1. The RcPYP* fully recovered to the preflash baseline in less than 10 ms, which is approximately 100 times faster than for HhPYP (compare to ref *2*).

Table 1: Rates of Recovery and Bleaching at Different Excitation and Detection Wavelengths for *Rhodobacter capsulatus* PYP[a]

	excitation at 445 nm	excitation at 386 nm	excitation at 365 nm
recovery, 440 nm	820 s^{-1}	628 s^{-1}	574 s^{-1}
bleach, 440 nm	2.0×10^4 s^{-1}	(not visible)	(not visible)
recovery, 375 nm			1100 s^{-1}
bleach, 375 nm			(not visible)

[a] Data were collected in universal buffer, pH 8.0, at room temperature.

cycles in which the recovery reaction of a component excited by 365 nm light is slightly faster than the 445 nm excited photocycle. A difference spectrum with time points taken 9 ms after the 365 nm flash gives results similar to those seen with the 386 nm excitation, with formation of the 435 nm form at the expense of the 375 nm form. We can see from Figure 8C that the ratio of "recovery above baseline" to bleach has increased to 0.50 with 365 nm excitation. This implies that, in fact, less of the 435 nm peak is bleached at the shorter excitation wavelength. Additionally, we can see from Figure 8B that the 375 nm form recovers to a new baseline, in this case slightly below the preflash baseline. These results indicate that during the excitation with 365

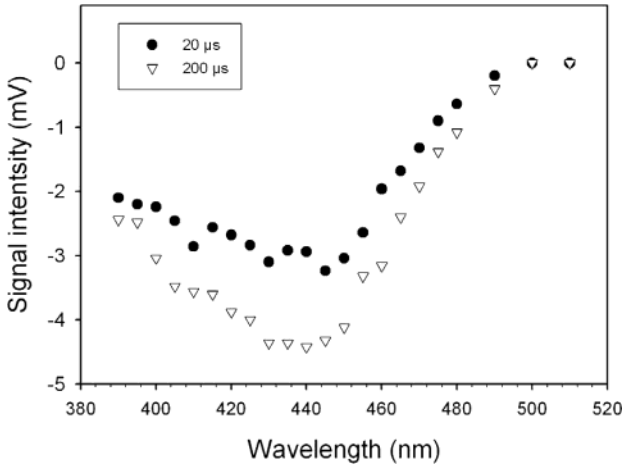

FIGURE 6: Difference absorption spectra of RcPYP* after 445 nm laser excitation. Black dots are data points taken after 20 μs, white triangles after 200 μs. Besides the expected bleaching of the 435 nm form, there is a shoulder around 410 nm which is visible after both 20 μs and 200 μs. Due to the high noise level, data points below 390 nm could not be accurately measured. The protein concentration is higher than that in the experiment of Figure 5.

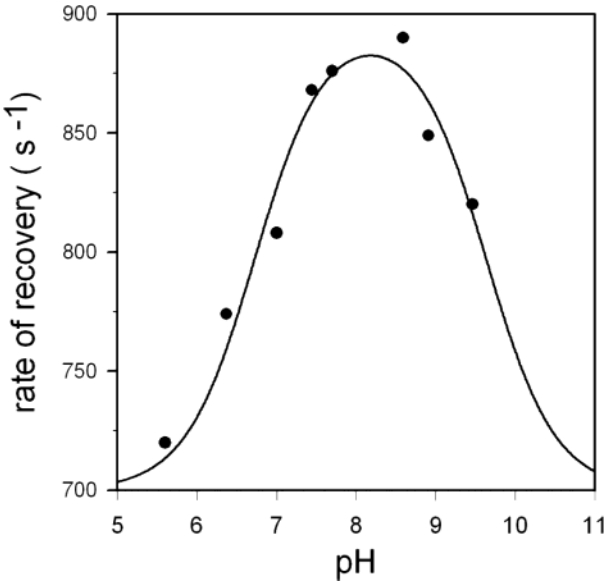

FIGURE 7: Effect of pH on the kinetics of the recovery reaction of RcPYP* after 445 nm laser excitation. The buffer consisted of 20 mM MES, 20 mM HEPES, and 20 mM glycine. Measurements were performed at room temperature. Precipitation of the sample interfered below pH 5.5. The pH effect on the kinetics appears to have a bell-shaped form, but is much less pronounced than for HhPYP. The data were fitted with the Henderson−Haselbach equation with two p*K*'s and with the two endpoints fixed at 700 s^{-1}. The resulting p*K* values are 6.7 and 9.6. The optimum rate constant was 890 s^{-1}.

nm, and also to a lesser extent with 386 nm laser light, a shorter wavelength absorbing form of RcPYP* can be converted into the 435 nm form. A similar result was previously observed with the RsPYP and attributed to a cis-protonated form of the chromophore (*22*).

Steady-state absorption experiments show that after repeatedly illuminating the sample for several minutes with 365 nm light as in the experiment described above, a large fraction of the 350−375 nm absorption is indeed converted into the 435 nm form. However, the 435 nm absorbance returns to the preflash baseline at room temperature, but it

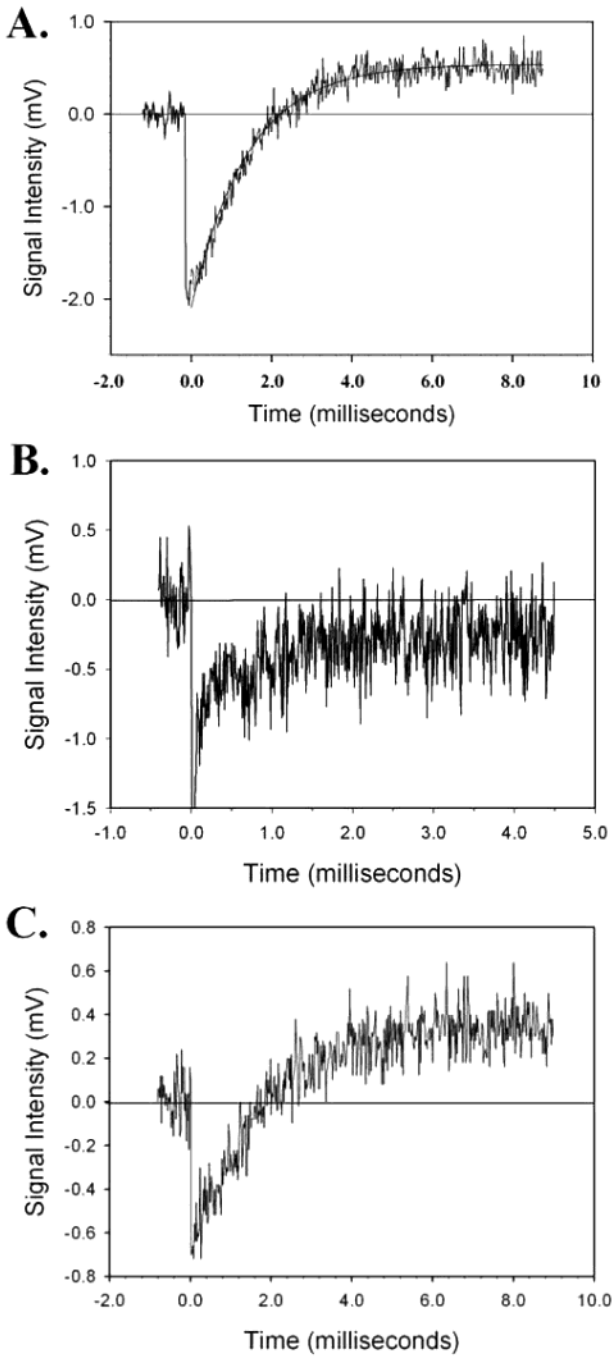

FIGURE 8: (A) Recovery of RcPYP* at 435 nm after excitation with 386 nm laser light (at time 0). After the bleach, RcPYP* recovers to a new baseline which is significantly higher than before the laser flash. (B) Recovery of RcPYP* after 365 nm laser light excitation, detected at 375 nm and (C) at 435 nm. In each, there is recovery to a new baseline, different from the preflash baseline. At 375 nm, the recovery is below the preflash baseline, while at 435 nm, the recovery ends above it. The ratio of "recovery above baseline" to bleach in (C) is higher than in (A). All measurements were performed in universal buffer, pH 8.0, at room temperature.

is a relatively slow process with an extrapolated half-life of 120−150 min. After overnight incubation in the spectrophotometer, the sample was almost completely denatured. In RsPYP, the excess 435 nm absorbance resulting from a laser flash at 330 nm recovered to the preflash baseline with a midpoint of approximately 25 min (*22*), i.e., 5−6 times faster than in RcPYP*.

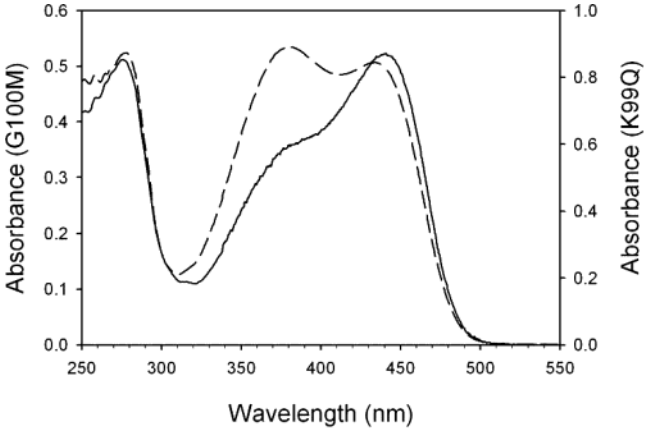

FIGURE 9: Absorption spectrum of the G100M (solid line) and the K99Q mutant (dashed line) of RcPYP* in Tris-HCl buffer (20mM, pH 9.0) at 10 °C. When compared to wild-type (Figure 2), the 375 nm absorption peak of the G100M mutant has significantly decreased in size. The 375 to 435 nm ratio of the K99Q mutant has not changed compared to wild-type (1.08 at 10 °C and pH 9.0).

Characterization of G100M and K99Q Mutants. Devanathan et al. (*31*) showed that the M100A mutation in HhPYP leads to a 1000-fold decrease in the recovery rate following flash illumination compared to wild-type PYP, suggesting that M100 facilitates the conversion of cis chromophore into the trans form. Both RsPYP and RcPYP have a naturally occurring G100 substitution, but surprisingly, their recovery to the ground state following a laser flash occurs 100-fold faster than for HhPYP (see above, and ref *4*). Another difference is that room light does not affect the 375 or 435 nm absorption amplitudes of either RsPYP or RcPYP*, as opposed to the M100A mutant of HhPYP. To further investigate this phenomenon, we mutated the Gly at position 100 in RcPYP* to a Met. The absorption spectrum of the mutant after purification is given in Figure 9. The 375 nm peak is clearly diminished but is still significant. At the same time, this diminished absorbance at 375 nm shifts the absorption maximum of 435 nm in wild-type RcPYP* to 441 nm in the G100M mutant. The 375 to 435−441 nm ratio has shifted from 1.0 for wild-type to 0.64 for G100M (at 20 °C, pH 9.0), which suggests that M100 has a role in stabilizing the longer wavelength absorbing form of PYP. This could result from a decrease in exposure of the chromophore to solvent in the G100M mutant. It does not necessarily indicate that the M100 is any closer to the chromophore in the ground state. However, the rate constants for bleach and recovery of G100M with different excitation wavelengths do not significantly vary from those of WT. This result is surprising, considering the large effect M100 has in HhPYP. In searching for an explanation for this phenomenon, we hypothesized that the nearby K99 in RcPYP* (Q99 in HhPYP) might also facilitate cis−trans isomerization by stabilizing partial negative charge at the two carbons of the double bond in the transition state. We thus constructed the K99Q mutation of RcPYP* and purified the protein as described for the wild-type. The absorption spectrum of K99Q (Figure 9) looks very much like that of wild-type RcPYP* and was not affected by exposure to room light or overnight incubation in the dark. Results of the flash photolysis experiments with K99Q RcPYP* also closely

resemble those of wild-type, which indicates that K99 does not have a significant role in the photocycle.

DISCUSSION

Protein Production and Purification. The *Rb. capsulatus pyp* gene was discovered by Jiang and Bauer (*5*), but the hypothetical PYP protein had not been characterized until now. The expression system we developed for *Hr. halophila pyp* through coexpression of the RcPYP biosynthetic genes (*19*) was also used here for the RcPYP. However, our initial attempts either with or without a His tag resulted in protein that was mostly colorless and insoluble. Incorporation of a glutathione-sulfur-transferase fusion had the desired effect of making the PYP more soluble and capable of binding chromophore. The GST tag was removed from purified protein in a subsequent treatment with thrombin, resulting in soluble PYP*. On the other hand, the closely related RsPYP was successfully produced as the apo-protein in the soluble state with a His tag, the PYP was chemically reconstituted with chromophore, and the His tag was subsequently removed (*4*). This suggests that the RsPYP is intrinsically more stable than RcPYP. The spectral properties, including the much larger absorbance ratio of 375 to 435 nm, the effects of denaturants in converting the 435 nm form to a shorter wavelength species, and the loss of color and precipitation below pH 5.5, also suggest that RcPYP* is less stable than is RsPYP since the latter only loses its color with a pK_a of 3.8 (*4*). In addition, about 50% of the purified RcPYP* does not redissolve when a sample is thawed after storage at −20 °C.

Spectral Properties. RcPYP* and RsPYP are spectrally similar in having two peaks at room temperature in pH 7 buffer. Although the ratio of 375 (or 360) to 435 (or 446) nm differs between Rc and Rs PYP (compare Figure 1 in ref *4* to the spectrum of purified RcPYP*), the two peaks show a significant temperature and pH dependence in both species, where the shorter wavelength form is favored at lower temperature and pH. The spectra are also similar to those of the HhPYP mutant Y42F that has an intermediate spectral form, which is also dependent on pH, but responds in the opposite way to temperature, that is, the shorter wavelength form is favored at higher temperature (*27*). It has been reported that WT HhPYP and mutants in the vicinity of the chromophore, except those with substitutions at position E46, can adopt an intermediate spectral form like that in Y42F, absorbing anywhere between 400 and 350 nm (*28*). It has been suggested that the chromophore in the intermediate spectral form is in an environment of higher and variable dielectric constant and that E46 may accept an additional hydrogen bond from a water molecule (*28*). However, this does not explain the inverse temperature effect in the *Rhodobacter* PYPs. It rather suggests that the 375 nm absorbance of RcPYP* may be a mixture of the intermediate spectral form first observed in HhPYP Y42F, because of the continuously variable wavelength, and a conformer which has the chromophore in the cis conformation (presumably with an absorbance maximum at 350 nm), because of the partial photoconversion of the shorter wavelength form to the longer wavelength form, as previously shown for RsPYP (*22*). If this is the case, it is probably the cis conformer which changes its conformation with temperature in the same way as in RsPYP. Additionally, we showed that the RcPYP* 435 and 375 nm absorbing forms are affected by both chaotropes and kosmotropes in a similar way as in the Y42F HhPYP mutant. Kosmotropes favor the 435 nm form, while in the presence of chaotropic salts it is disfavored. At high concentrations of chaotrope, the RcPYP* changes its two characteristic absorption peaks to a form absorbing at 350 nm, which corresponds to fully protonated chromophore that is presumably exposed to solvent. While kosmotropes are known to "salt out" hydrophobic residues and therefore are generally used as protein stabilizers, chaotropes interact with the charged groups and dipoles of proteins and, in this way, reduce the number of water clusters in the first hydration shell ("salting in"), resulting in destabilization of the protein (*32*).

Kinetic Properties. It was reported that the RsPYP is bleached more rapidly by a laser flash than is HhPYP and that the recovery is also 100-fold faster (*4*). We found that the RcPYP* is bleached 10-fold faster by a laser flash at 445 nm and that the recovery is 100-fold faster than in HhPYP. Thus, Rc and RsPYP appear to be similar in this regard. It was previously shown that the HhPYP mutant M100A has a very slow recovery, being 1000-fold less than for WT protein (*15*). This was ascribed to catalysis of cis−trans isomerization by the polarizable Met100 sulfur, which resides over the chromophore aromatic ring in the I_2 intermediate. That is, the electron-rich sulfur can stabilize the partial positive charge on the aromatic ring in the transition state. Although the slow recovery could also be due to destabilization of the protein, other destabilizing mutations do not affect the recovery kinetics so dramatically (*9*). Additional HhPYP mutations at position M100, such as M100L, behave similarly to M100A (*33*), which indicates that the slower recovery effect is specifically due to loss of the thioether moiety of M100 and not solely to reduced stability. Both RsPYP and RcPYP* proteins have G100 substitutions, which were expected to result in significantly slower, not faster, recovery. It has been suggested that T50A and V66I substitutions in RcPYP* and RsPYP relative to HhPYP, in addition to the M100G substitution, might result in greater exposure of the chromophore to solvent (*22*). However, based on the presented kinetic results, it is unknown what compensating substitutions may have occurred to speed up the recovery in the *Rhodobacter* species studied.

We found that the G100M mutant of RcPYP* has an absorption spectrum similar to that of wild-type but that the 441 nm peak is more pronounced, which suggests that M100 has a stabilizing function in shifting the equilibrium toward the longer wavelength form. In both Rs and RcPYP*, there is a K99 residue, spatially close to G100, which might also reside over the chromophore and stabilize the partial negative charge on the chromophore double bond to catalyze the isomerization. However, the K99Q mutant of RcPYP* has virtually the same absorption spectrum as WT, yet it was not sensitive to room light as was the case with HhPYP M100A, and it had recovery kinetics similar to those of wild-type RcPYP*. This suggests that neither K99 nor M100 catalyzes isomerization of the chromophore in these species. This may be a result of the protein adopting a different conformation of the loop containing these residues, which is distinct from the conformation in HhPYP (*13*) and *R.*

centenaria Ppr (*34*), that results in very fast recovery of Rc and RsPYPs.

When the RcPYP* is excited by shorter wavelength laser light at 386 or 365 nm, the kinetics monitored at 435 nm do not change appreciably, but the end point of the recovery is above the preflash baseline, more so for 365 nm light than for 386 nm light. This is different from the HhPYP Y42F mutant, which shows identical behavior with 365 nm excitation and with 445 nm excitation (*27*), but is similar to what was recently reported for RsPYP (*22*). Combining the spectral and kinetic studies, the simplest model is one with three species in the dark state. These would include the 440 nm conformer, the 375 conformer, and a population containing the cis form of the chromophore (presumably absorbing at 350 nm). When excited by a laser flash, the 375 and 440 nm conformers bleach, forming a cis form which then recovers in the dark with a rate constant in the 600−800 s^{-1} range. The cis form present in the dark is converted by light excitation to a trans form which absorbs in the 440 nm region and decays with a half-life of about 2 h.

The amount of cis conformation chromophore in WT HhPYP is too small to be measured, and the dark equilibrium for mutant M100A is also in favor of the trans form. However, we believe that it is the equilibrium between the cis and trans chromophores that is uniquely affected by temperature in the Rc and RsPYP. That is, an increase in temperature converts the cis form (absorbing at 350 nm) to the 440 nm absorbing species. It remains to be determined how similar the cis form may be to the photoproduced I_2 intermediate, which is also in the cis conformation and exposed to solvent. Because the recovery above baseline is larger with 365 nm than for 386 nm excitation and is virtually nonexistent with 445 nm excitation, we believe that the postulated cis form is also protonated and absorbs closer to 350 nm than to 375 nm. Thus, the kinetics with 445 nm excitation may be dominated by the normal bleach/recovery at 375/440 nm. However, the chromophore in the cis conformation, which is photoisomerized by excitation at shorter wavelengths, has faster kinetics than the normal recovery. That there is indeed a dark temperature-dependent equilibrium between cis and trans conformations is shown by the fact that the excess 435 nm absorbance produced by a laser flash at short wavelengths in RcPYP* only slowly returns to the preflash baseline over a period of hours. This occurs significantly faster in RsPYP than in RcPYP*. The results suggest that the differences in energy levels for the three forms of RcPYP* are smaller and that the trans form of the chromophore can switch to the cis form in the dark more readily than in HhPYP.

RsPYP can also be photoexcited at 360 nm (*22*), with some of the results being very similar to those obtained with RcPYP*, although they were interpreted in a different way. The 360 nm form was proposed to be different from the HhPYP Y42F 391 nm shoulder, and when excited with 360 nm light gives rise to a new 435 nm form which was said to be different from the ground state 446 nm form. The 435 nm species returns back to the 360 nm form in a few minutes. Essentially, it was proposed that there are two photocycles in this PYP (one initiated by 445 nm excitation and one by UV-light excitation (330 ± 50 nm)) that occur independently. Surprisingly, when the photocycle kinetics were studied at 446 nm, an incomplete recovery of the RsPYP to the preflash baseline after 445 nm excitation was seen. The incomplete recovery was attributed to an unintended photoactivation of the 360 nm (second) photocycle, and by using a 450 ± 7 nm band-pass filter, the recovery could be brought to completion. If the same were true for RcPYP*, then incomplete recovery would be expected to be even more pronounced, since the 375 and 435 nm peaks have greater overlap. On the contrary, in the RcPYP* experiments, the recovery was fully complete within 10 ms (see Figure 5B).

Further experiments with RcPYP* will have to be conducted to determine whether the excess 435 nm absorption seen after 365 nm excitation is truly the 435 nm absorbing form of the ground state as we propose, or whether it is a new species with a similar absorption spectrum which cannot be resolved, as proposed for the 360 nm photocycle of RsPYP. In other words, the two photocycles may not be independent and a light-induced conversion of one ground state to the other might occur as in the HhPYP M100A mutant. Due to the energy barrier between the two ground states, a return to the prestimulus level would occur through a slow (e.g., overnight) dark process. Regardless of the mechanistic details, it is clear that RsPYP and RcPYP* both show particular features that appear to be restricted to this subgroup of the PYP family, such as the presence of a significant amount of intermediate spectral form in the WT protein, the presence of a dark cis/trans equilibrium, and a unique mechanism for recovery.

Genetic Context of PYP. Besides these spectral and kinetic distinctions, we found that the genes for PYP, TAL, and pCL are clustered with 9−13 genes for gas vesicle formation in *Rb. capsulatus*. The gene for TAL is clustered with the same *gvp* genes in the same orientation in *Rb. sphaeroides* strain 2.4.1. Apparently, the genes for PYP and pCL have been deleted through years of nonselective growth of this strain. To our knowledge it is not known that any *Rhodobacter* species are capable of producing gas vesicles, and until recently no observations were made of gas vesicles in any purple nonsulfur bacteria (*35*). It remains to be determined whether and under what circumstances PYP or the *gvp* genes may be expressed in *Rhodobacter* species. Gas vesicle formation has been studied more thoroughly in halobacterial species than in any other (*36*). However, the transcriptional regulators *gvpE* and *gvpD*, found in *Haloferax volcanii* (*37*), seem to be absent in *Rhodobacter*, nor is there a PYP in halobacteria based upon BLAST searches. Anaerobic conditions, darkness, and stationary growth stage favor gas vesicle formation in the halobacteria and should also favor their formation in *Rhodobacter*, which is both photosynthetic and aerobic. We postulate that *Rhodobacter* gas vesicles and PYP are also produced under similar conditions and that PYP acts as a transcriptional repressor under high light conditions. We are currently testing these hypotheses through the use of reporter genes.

CONCLUSIONS

1. The RcPYP is less stable but has spectral and kinetic properties similar to those of RsPYP, both of which are significantly different from HhPYP and near homologues. This indicates that the *Rhodobacter* PYPs constitute a subgroup distinct from that of the three halophiles, which have virtually identical spectral and kinetic properties despite large sequence differences.

2. The faster recovery following illumination in *Rhodobacter* PYPs indicates that higher light intensity is necessary to maintain the same steady-state concentration of the signaling state; i.e., it is less sensitive to light quantity than in the halophiles. However, the broader wavelength maxima indicate that it is more sensitive to light quality, both of which suggest that the functional role may be different.

3. The conformation of the beta 4−5 loop, which contains residues K99 and M100, is different in the *Rhodobacter* PYPs, as indicated by mutagenesis, and this suggests a distinct functional role. This loop is thought to be important because it is located at the gateway for isomerization of the chromophore.

4. The observation of gas vesicle genes and their association with those for PYP in the *Rhodobacter* species as well as known regulation of *gvp* by light in other species suggests that the role of PYP is in regulation of cell buoyancy.

REFERENCES

1. Meyer, T. E. (1985) Isolation and characterization of soluble cytochromes, ferredoxins and other chromophoric proteins from the halophilic phototrophic bacterium *Ectothiorhodospira halophila*, *Biochim. Biophys. Acta 806*, 175−183.
2. Meyer, T. E., Yakali, E., Cusanovich, M. A., and Tollin, G. (1987) Properties of a water-soluble, yellow protein isolated from a halophilic phototrophic bacterium that has photochemical activity analogous to sensory rhodopsin, *Biochemistry 26*, 418−423.
3. Koh, M., van Driessche, G., Samyn, B., Hoff, W. D., Meyer, T. E., Cusanovich, M. A., and Van Beeumen, J. J. (1996) Sequence evidence for strong conservation of the photoactive yellow proteins from the halophilic phototrophic bacteria *Chromatium salexigens* and *Rhodospirillum salexigens*, *Biochemistry 35*, 2526−2534.
4. Haker, A., Hendriks, J., Gensch, T., Hellingwerf, K., and Crielaard, W. (2000) Isolation, reconstitution and functional characterization of the *Rhodobacter sphaeroides* photoactive yellow protein, *FEBS Lett. 486*, 52−56.
5. Jiang Z., and Bauer C. E. (1998) Genetic characterization of photoactive yellow protein from *Rhodobacter capsulatus* (direct submission to GenBank, accession no. AF064095).
6. Jiang, Z., Swem, L. R., Rushing, B. G., Devanathan, S., Tollin, G., and Bauer, C. E. (1999) Bacterial photoreceptor with similarity to photoactive yellow protein and plant phytochromes, *Science 285*, 406−409.
7. Kyndt, J. A. (2003) Ph.D. Thesis, University of Gent, Gent, Belgium.
8. Pellequer, J., Wager-Smith, K. A., Kay, S. A., and Getzoff, E. D. (1998) Photoactive yellow protein: A structural prototype for the three-dimensional fold of the PAS domain superfamily, *Proc. Natl. Acad. Sci. U.S.A.* 95, 5884−5890.
9. Cusanovich M. A., and Meyer T. E. (2003) Photoactive yellow protein: a prototypic PAS domain sensory protein and development of a common signaling mechanism. *Biochemistry 42*, 4759−4770.
10. Baca, M., Borgstahl, G. E. O., Boissinot, M., Burke, P. M., Williams, D. R., Slater, K. A., and Getzoff, E. D. (1994) Complete chemical structure of photoactive yellow protein: novel thioester-linked 4-hydroxycinnamyl chromophore and photocycle chemistry, *Biochemistry 33*, 14369−14377.
11. Hoff, W. D., Düx, P., Hard, K., Devreese, B., Nugteren-Roodzant, I. M., Crielaard, W., Boelens, R., Kaptein, R., Van Beeumen, J. J., and Hellingwerf, K. J. (1994) Thiol ester-linked *p*-coumaric acid as a new photoactive prosthetic group in a protein with rhodopsin-like photochemistry, *Biochemistry 33*, 13959−13962.
12. Van Beeumen, J. J., Devreese, B., Van Bun, S., Hoff, W. D., Hellingwerf, K. J., Meyer, T. E., McRee, D. E., and Cusanovich, M. A. (1993) Primary structure of a photoactive yellow protein from the phototrophic bacterium *Ectothiorhodospira halophila*, with evidence for the mass and the binding site of the chromophore, *Protein Sci. 2*, 1114−1125.
13. Borgstahl, G. E. O., Williams, D. R., and Getzoff, E. D. (1995) 1.4 Å structure of photoactive yellow protein, a cytosolic photoreceptor: unusual fold, active site, and chromophore, *Biochemistry 34*, 6278−6287.
14. Ujj, L., Devanathan, S., Meyer, T. E., Cusanovich, M. A., Tollin, G., Atkinson, G. H. (1998) New photocycle intermediates in the photoactive yellow protein from *Ectothiorhodospira halophila*: picosecond transient absorption spectroscopy, *Biophys. J. 75*, 406−412.
15. Devanathan, S., Pacheco, A., Ujj, L., Cusanovich, M. A., Tollin, G., Lin, S., and Woodbury, N. (1999) Femtosecond spectroscopic observations of initial intermediates in the photocycle of the photoactive yellow protein from *Ectothiorhodospira halophila*. *Biophys. J. 77*, 1017−1023.
16. Rubinstenn, G., Vuister, G. W., Mulder, F. A. A., Düx, P. E., Boelens, R., Hellingwerf, K. J., and Kaptein, R. (1998) Structural and dynamic changes of photoactive yellow protein during its photocycle in solution. *Nature Struct. Biol. 5*, 568−570.
17. Borucki, B., Devanathan, S., Otto, H., Cusanovich, M. A., Tollin, G., and Heyn, M. P. (2002) Kinetics of proton uptake and dye binding by photoactive yellow protein in wild type and in the E46Q and E46A mutants. *Biochemistry 41*, 10026−10037.
18. Haselkorn, R., Lapidus, A., Kogan, Y., Vlcek, C., Paces, J., Paces, V., Ulbrich, P., Pecenkova, T., Rebrekov, D., Milgram, A., Mazur, M., Cox, R., Kyrpides, N., Ivanova, N., Kapatral, V., Los, T., Lykidis, A., Mikhailova, N., Reznik, G., Vasieva, O., and Fonstein, M. (2002) The *Rhodobacter capsulatus* genome, *Photosynth. Res. 70*, 43−52.
19. Kyndt, J. A., Vanrobaeys, F., Fitch, J. C., Devreese, B. V., Meyer, T. E, Cusanovich, M. A., and Van Beeumen, J. J. (2003) Heterologous production of *Halorhodospira halophila* holo photoactive yellow protein through tandem expression of the postulated biosynthetic genes, *Biochemistry 42*, 965−970.
20. Imamoto, Y., Ito, T., Kataoka, M., and Tokunga, F. (1995) Reconstitution of photoactive yellow protein from apoprotein and p-coumaric acid derivatives, *FEBS Lett. 374*, 157−160.
21. Genick, U. K., Devanathan, S., Meyer, T. E., Canestrelli, I. L., Williams, E., Cusanovich, M. A., Tollin, G., and Getzoff, E. D. (1997) Active site mutants implicate key residues for control of color and light cycle kinetics of photoactive yellow protein, *Biochemistry 36*, 8−14.
22. Haker, A., Hendriks, J., van Stokkum, I. H. M., Heberle, J., Hellingwerf, K. J., Crielaard, W., and Gensch, T. (2003) The two photocycles of photoactive yellow protein from *Rhodobacter sphaeroides*, *J. Biol. Chem. 278*, 8442−8451.
23. Sambrook, J., Fritsch, E. F., and Maniatis, T. (1989) *Molecular cloning: a laboratory manual*, 2nd ed., Cold Spring Harbor Laboratory Press, Cold Spring Harbor, NY.
24. Simondsen, R. P., and Tollin, G. (1983) Transient kinetics of redox reactions of flavodoxin: effects of chemical modification of the flavin mononucleotide prosthetic group on the dynamics of intermediate complex formation and electron transfer, *Biochemistry 22*, 3008−3016.
25. Offner, S., Hofacker, A., Wanner, G., and Pfeifer, F. (2000) Eight of the fourteen *gvp* genes are sufficient for formation of gas vesicles in halophilic Archaea. *J. Bacteriol. 182*, 4328−4336.
26. Mihara, K., Hisatomi, O., Imamoto, Y., Kataoka, M., and Tokunaga, F. (1997) Functional expression and site-directed mutagenesis of photoactive yellow protein, *J. Biochem. 121*, 876−880.
27. Brudler, R., Meyer, T. E., Genick, U.K., Devanathan, S., Woo, T. T., Millar, D. P., Gerwert, K., Cusanovich, M. A., Tollin, G., and Getzoff, E. D. (2000) Coupling of hydrogen bonding to chromophore conformation and function in photoactive yellow protein, *Biochemistry 39*, 13478−13486
28. Meyer, T. E., Devanathan, S., Woo, T., Getzoff, E. D., Tollin, G., and Cusanovich, M. A. (2003) Site-specific mutations provide new insights into the origin of pH effects and alternative spectral forms in the photoactive yellow protein from *Ectothiorhodospira halophila*, *Biochemistry 42*, 3319−3325.
29. Meyer, T. E., Tollin, G., Hazzard, J. H., and Cusanovich, M. A. (1989) Photoactive yellow protein from the purple phototrophic bacterium, *Ectothiorhodospira halophila*, *Biophys. J. 56*, 559−564.
30. Van Brederode, M. E., Hoff, W. D., Van Stokkum, I. H. M., Groot, M.-L., and Hellingwerf, K. J. (1996) Protein folding thermodynamics applied to the photocycle of the photoactive yellow protein, *Biophys. J. 71*, 365−380.
31. Devanathan, S., Genick, U.K., Canestrelli, I. L., Meyer, T. E., Cusanovich, M. A., Getzoff, E. D., and Tollin, G. (1998) New insights into the photocycle of *Ectothiorododspira halophila* photoactive yellow protein: Photorecovery of the long-lived

photobleached intermediate in the Met100Ala mutant, *Biochemistry 37*, 11563−11568.
32. Baldwin, R. L. (1996) How Hofmeister ion interactions affect protein stability, *Biophys. J. 71*, 2056−2063.
33. Kumauchi, M., Hamada, N., Sasaki, J., and Tokunaga, F. (2002) A role of methionine 100 in facilitating PYP_M decay process in the photocycle of photoactive yellow protein, *J. Biochem. 132*, 205−210.
34. Rajagopal, S., and Moffat, K. (2003) Crystal structure of a photoactive yellow protein from a sensor histidine kinase: conformational variability and signal transduction, *Proc. Natl. Acad. Sci. U.S.A. 100*, 1649−1654.
35. Karr, E. A., Sattley, W. M., Jung, D. O., Madigan, M. T., and Achenbach, L. A. (2003) Remarkable diversity of phototrophic purple bacteria on a permanently frozen antarctic lake, *Appl. Environ. Microbiol. 69*, 4910−4914.
36. Walsby, A. E. (1994) Gas vesicles, *Microbiol. Rev. 58*, 94−144.
37. Pfeifer, F., Gregor, D., Hofacker, A., Ploesser, P., and Zimmermann, P. (2002) Regulation of gas vesicle formation in halophilic archaea, *J. Mol. Microbiol. Biotechnol. 4*, 175−181.

BI035789F